analytical chemistry

pubs.acs.org/ac Article

Nanoprecipitation-Enhanced Sensitivity in Enzymatic Nanofluidic Biosensors

Ana S. Peinetti,* M. Lorena Cortez, Maria Eugenia Toimil-Molares, and Omar Azzaroni*

Cite This: *Anal. Chem.* 2024, 96, 5282−5288 Read Online

ACCESS | Metrics & More | Article Recommendations | Supporting Information

ABSTRACT: Single nanochannels show unique transport properties due to nanoconfinement. It has been demonstrated that at submillimolar concentrations of divalent cations, a nanoprecipitation reaction can occur in nanochannels. Although several reports have shown, described, and modeled the nanoprecipitation process, no further advantages have been taken from this phenomenon. Here, we show that the nanoprecipitation reaction can be incorporated into enzyme-modified nanochannels to enhance the performance of small-molecule biosensors via in situ amplification reactions. Contrary to the working principle of previous enzymatic nanofluidic biosensors, the nanofluidic biosensor described in this work operates on the basis of concerted functions: pH-shifting enzymatic activity and nanoprecipitation. We show that the simple addition of Ca^{2+} and Mg^{2+} ions in the working analyte solution containing urea can lower the detection limit from the nanometer to the subnanometer regime and modulate the dynamic linear range. This approach enables the implementation of more sensitive real-time nanofluidic detection methods without increasing the complexity of the nanofluidic platform or the sensing approach. We envision that the integration of concerted functions in nanofluidic architectures will play a key role in expanding the use of these nanoscale devices for analytical purposes.

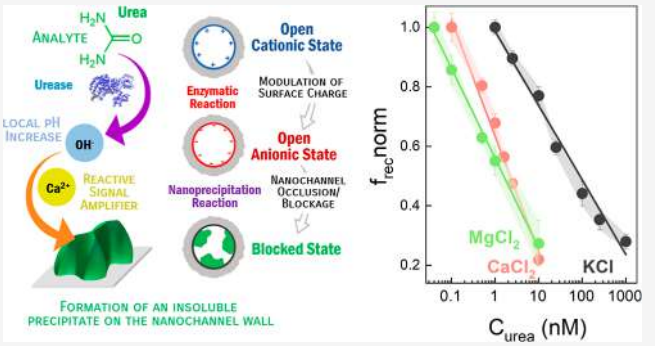

INTRODUCTION

Single nanochannels show unique transport properties and have attracted great interest in the scientific community as a model system to study ionic and molecular transport at the nanoscale,[1−4] as well as nanofluidic devices for real-world applications, such as biosensors, molecular filtration, and energy conversion.[5−13] In nanofluidic systems, the transport of ionic and molecular species in highly confined environments occurs upon the application of electrical fields. Early results showed that unique phenomena, such as unipolar conductivity, ionic rectification, and molecular sieving by size and charge, arise from this confinement.

To date, different reports that leverage the confinement effects have achieved ultrahigh sensitivity with solid-state nanopores/nanochannels biosensors by combining nanofabrication with surface modification techniques.[14,15] In particular, enzymatic architectures have attracted a considerable amount of attention. In these systems, the immobilized enzyme catalyzes specific biochemical reactions that can change the charge of the pore by changing the charge of the enzyme,[16,17] or for instance, catalyzing a reaction that changes the local pH in the nanochannel.[18] These changes are generally subtle in bulk materials; however, in nanochannels, they produce significant differences in the rectification properties. Thus, nanochannel properties can be harnessed to design sensitive sensors. Moreover, for sensing architectures, Matile and collaborators[19] incorporated the concept of reactive amplifiers, i.e., molecules that can react with the functional group created during enzymatic signal generation, providing stronger pore blocking or pore charge and thus enabling the sensing of otherwise overlooked analytes. These reactive amplifiers were conceived conceptually as reactions in situ without significant additional effort. We have demonstrated in previous works[18,20] the use of polyelectrolytes in nanochannels as "reactive signal amplifiers". In this configuration, we electrostatically assembled cationic weak polyelectrolytes, such as poly(allylamine) or poly(ethylenimine), on the anionic surface of asymmetrically shaped nanochannels. These polyelectrolytes play a key role as a "reactive signal amplifier" as they enhance the variations in the nanochannel surface charge due to the pH-shifting enzymatic process and enable nanomolar detection of relevant small molecules such as urea (1 nM LoD)[18] and acetylcholine (16 nM LoD).[20] Moreover, we showed that the polyelectrolyte leads to a zwitterionic pore

Received: January 10, 2024
Revised: March 4, 2024
Accepted: March 7, 2024
Published: March 21, 2024

https://doi.org/10.1021/acs.analchem.4c00203
Anal. Chem. 2024, 96, 5282−5288

Scheme 1. Representation of the Working Principle of Enzymatic Nanofluidic Biosensors Whose Sensitivity Is Enhanced by a Nanoprecipitation Process[a]

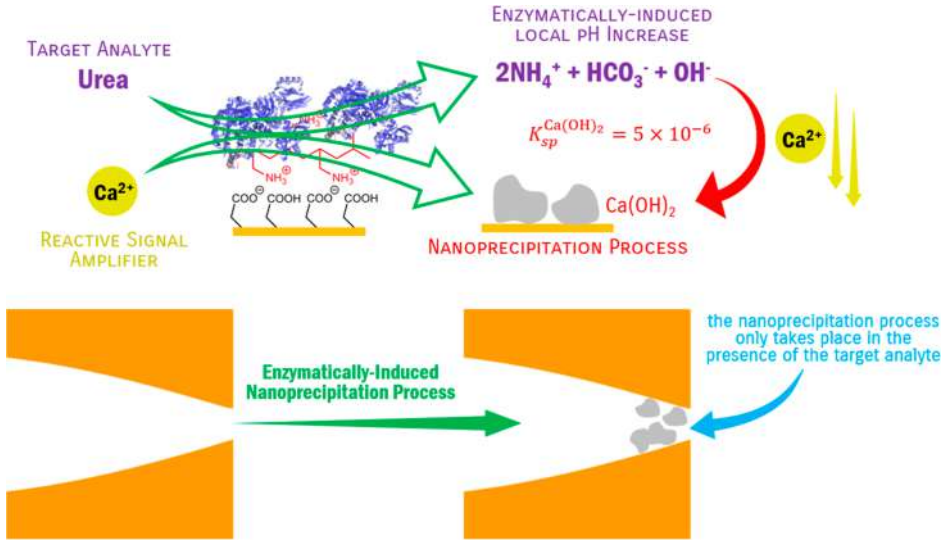

[a]The amplified detection of the analyte is achieved by the precipitation of the insoluble material on the enzyme-modified nanochannel.

wall that can be modulated by the enzymatic process in such a way that the responsive nanofluidic device displays fully reversible ionic rectification.

Because of their pore sizes of a few nanometers, the high surface-to-volume ratio in nanochannels can significantly affect mass transport, producing concentration enhancement and depletion of solution at the opening of nanochannels relative to bulk. Siwy and others have described a phenomenon occurring in nanopores/nanochannels called nanoprecipitation,[21−25] characterized by the transient formation of precipitates in the nanochannel opening. If the solution contains monovalent cations, such as K^+, the ions flow through the pore, establishing a constant ionic current. However, if the solution contains submillimolar concentrations of divalent cations, such as Ca^{2+}, Co^{2+}, or Mg^{2+}, the ionic current is not constant but oscillates, reflecting a sequence of low and high conductance states.[23,24,26] The low conductance state is caused by a precipitate getting clogged in the nanopore, obstructing the ion flow, while the high conductance state is caused by the dissolution of the precipitate, resetting the ion flow. Key players are the carboxyl groups exposed at the nanopore surface. When deprotonated, carboxyl groups retain divalent cations and act as nucleation centers for precipitation. The precipitate grows around carboxyl groups, blocking the pore entrance and decreasing the flow of ions through the pore. Although several reports have shown, described, and modeled the nanoprecipitation process, no further advantages have been taken from this process in terms of application.

In this work, we propose for the first time the use of divalent cations as "reactive signal amplifiers" in nanofluidic enzymatic biosensors, taking advantage of the nanoprecipitation reaction that occurs in nanochannels when millimolar concentrations of divalent cation are present.[27] In particular, we show that divalent cations can be used as a "reactive signal amplifier," controlling nanoprecipitation inside the nanopore and tuning the iontronic signal, and therefore the dynamic range and sensitivity of nanochannel biosensors operating via pH-shifting enzymatic processes. In this regard, our conceptual paradigm relies on the simple addition of divalent cations, such as Ca^{2+} or Mg^{2+}, to the working electrolyte solution containing the analyte in order to promote the formation of a nanoprecipitate on the nanochannel tip resulting from the pH variation due to the enzymatic processes. Ultimately, this concerted process (enzymatic activity + nanoprecipitation) leads to an enhancement in the sensitivity of the enzymatic nanochannel sensors as it increases the variations in the nanochannel surface charge and the excluded volume, i.e., effective nanochannel cross-section, after the pH-shifting enzymatic process occurs in the presence of the target analyte. The proposed paradigm is represented in Scheme 1.

MATERIALS AND METHODS

Materials. Poly(allylamine) hydrochloride (PAH), potassium chloride, and calcium chloride were purchased from Sigma-Aldrich, urease from *Canavalia ensiformis* (Jack bean) from Calzyme, and surfactant Dowfax 2A1 from Dow Chemicals. All of these reactants were used as received. Poly(ethyleneterephthalate) (PET) foils (Hostaphan RN 12, Hoechst) of 12 μm thickness were irradiated with 2.2 GeV Au ions at the UNILAC accelerator of the GSI Helmholtzzentrum für Schwerionenforschung GmbH (Darmstadt, Germany).

Nanochannel Fabrication. By chemical hydrolysis, i.e., etching, the cylindrical volume of damage created by each ion along its path, called ion track, can be selectively removed.[35,36] The etching is performed by inserting the irradiated polymer foil between two compartments of a chemical cell. One compartment is filled with 6 M NaOH solution and the other one with 6 M NaOH + 0.05% (v/v) Dowfax 2a1. After 6 min of etching at 60 °C, the polymer foil is rinsed carefully with distilled water. The nanochannels exhibit a so-called bullet-like shape consisting of a cylindrical and a parabolic segment, with the vertex pointing toward the solution with surfactant. These nanochannels display nonlinear current−voltage characteristics due to their asymmetric shape and the negative charges stemming from the carboxylate groups generated on the surface after the hydrolysis.[1]

Modification with PAH and Urease. After the etching procedure, the nanochannel-containing foils were modified by

https://doi.org/10.1021/acs.analchem.4c00203
Anal. Chem. 2024, 96, 5282−5288

dip-coating with PAH and urease, as reported previously.[18] PAH was incorporated by dip-coating in a 10 mM solution of PAH (in monomer units) at pH 6 for 1 h. Then, urease was integrated into the PAH-modified nanochannel by dip-coating in a urease solution (1 mg/mL in 10 mM HEPES buffer +10 mM KCl, pH 7.4).

Current−Voltage Characteristics. Current−voltage curves were measured using a commercially available potentiostat (Gamry—Reference 600) in a four-electrode setup (working, working sense, reference, and counter-electrode). In this way, we can measure conductance variations arising from changes in the nanochannel and not from other processes in solution or electrode surfaces. Both the working and counter electrodes were platinum wires, while the reference and working-sense electrodes were commercial silver/silver chloride (Ag/AgCl/3 M KCl) electrodes. The conductivity cell comprises two compartments, separated by a single nanochannel membrane and designed to avoid leakage currents while measuring. In all the experiments, the working electrode was placed at the base of the nanochannel while the counter-electrode was placed at the tip. A 0.1 M KCl solution was used as the electrolyte. To test the nanoprecipitation effect, a combination of 10 mM of $CaCl_2$ with 0.1 M KCl or 10 mM $MgCl_2$ with 0.1 M KCl solution was used as the electrolyte.

To measure the pH dependence, NaOH or HCl solution drops were added to adjust the different pH values to the electrolyte solution. All of the pH values were measured with a pH meter.

Rectification Factor (f_{rec} and f_{rec}norm). The rectification factor (f_{rec}) is defined as

$$f_{rec} = \pm \left| \frac{I(1\ \text{V or } -1\ \text{V})}{I(-1\ \text{V or } 1\ \text{V})} \right| \quad (1)$$

where the current I in the numerator corresponds to the largest current value in the high conductance state, whereas the current in the denominator is the lowest current value corresponding to the low conductance state. Additionally, if the higher current corresponds to a negative voltage, then the rectification factor is multiplied by −1. This definition allows assigning a negative f_{rec} for the case of a negatively charged nanochannel and a positive f_{rec} for a positively charged one. This definition simplifies the notation and allows the discussion of experimental results in terms of surface charge. To compare results stemming from different nanochannels, a normalized rectification efficiency (f_{rec}norm) was defined by dividing each f_{rec} from a specific nanochannel by its highest f_{rec} value (f_{rec}max)

$$f_{rec}\text{norm} = \frac{f_{rec}}{|f_{rec}\text{max}|} \quad (2)$$

RESULTS AND DISCUSSION

To explore the possibility of using divalent cations as "reactive signal amplifiers" in nanochannel-based sensors, we have chosen Ca^{2+} and Mg^{2+} cations. Siwy and collaborators demonstrated that weakly soluble compounds, such as $CaHPO_4$, $CoHPO_4$, and $Mg(OH)_2$, can precipitate inside a single nanochannel with a negative surface charge.[21,22] Vilozny et al. have shown that cations with low solubility show the formation of reversible precipitate in quartz nanopipettes, but extremely low-soluble precipitates like iron hydroxide [K_{sp} $Fe(OH)_3 = 10^{-39}$] irreversibly block the nanopore.[24] By choosing Ca^{2+} and Mg^{2+} cations to investigate the nanoprecipitation reaction, we expect them to have a high chance of forming reversible precipitates due to the formation of relatively soluble precipitates [K_{sp} $Ca(OH)_2 = 5 \times 10^{-6}$, K_{sp} $Mg(OH)_2 = 1 \times 10^{-11}$].

To test our hypothesis, we prepared PAH-modified single-nanochannel membranes based on previously reported protocols.[18] Briefly, PET films are irradiated with single swift heavy ions, followed by chemical etching of the generated single-ion nanochannels. Then, the nanochannels are modified with PAH via electrostatic self-assembly. This PAH-modified PET nanochannel produces an "amphoteric"[28,29] highly charged surface that generates a pH-dependent behavior of the rectification factor when the current−voltage (I vs V) curve is measured in the presence of 0.1 M KCl. We have shown that when pH is lower than pH 7, the surface is positively charged due to protonation of NH_2 groups, while at pH 9, the rectification direction changes showing an inversion to negative surface charge due to deprotonation of carboxylate groups.[18] In this PAH−PET nanochannel, we incorporated urease. Previously, we demonstrated that different concentrations of urea in a urease−PAH−PET nanochannel produce a local change in the pH and, thus, a change in the protonation state of the nanochannel due to the enzymatic reaction of urea in the presence of urease that produces ammonium and hydroxyl ions. Then, a sensitive detection of urea can be achieved with a LoD of 1 nM.[18] Within this framework, we consider that this well-characterized system is an excellent platform to evaluate the use of divalent cations as reactive amplifiers, enabling the fine-tuning of analytical parameters of nanofluidic biosensors.

First, we studied the effect of divalent Ca^{2+} ions on the ion current rectification properties of a urease−PAH−PET nanochannel by measuring the I vs V curve in the absence and presence of $CaCl_2$ at different pH values. Figure S1 shows the results of the I vs V curve measured in 0.1 M KCl and in 0.1 M KCl with 10 mM Ca^{2+}. In both cases, the pH was adjusted to different values between 5 and 9 by the dropwise addition of NaOH or HCl to reach each pH value. Based on the I vs V curves, we calculated the rectification factor (f_{rec}), defined as the ratio between the current at 1 V and the current at −1 V (eq 1, Materials and Methods). Then, for comparison between different nanochannels, the rectification factor (f_{rec}) was normalized by dividing each value by the maximum absolute value obtained for a given nanochannel (eq 2, Materials and Methods). Figure 1 shows the normalized rectification factor (f_{rec}norm) vs pH. It can be observed that changing the pH from acidic to basic conditions in the electrolyte solution (0.1 M KCl, without Ca^{2+}) leads to the reversion of the rectification direction and consequently to the reversion in the selectivity of the channel, as expected due to the "amphoteric" behavior of urease−PAH−PET nanochannel. Then, when 10 mM Ca^{2+} solution is incorporated into the electrolyte solution, a change in the behavior is observed. At pH > 7, in the presence of Ca^{2+}, no inversion of rectification properties is seen. Instead, the f_{rec}s are always close to 1. This result is in agreement with nanoprecipitation of $Ca(OH)_2$ taking place at a pH higher than 7, blocking the nanochannel as reported.[24]

To confirm the effect of the divalent cation, we tested with another cation, Mg^{2+}.[30] Figure 1 shows the dependence of

https://doi.org/10.1021/acs.analchem.4c00203
Anal. Chem. 2024, 96, 5282−5288

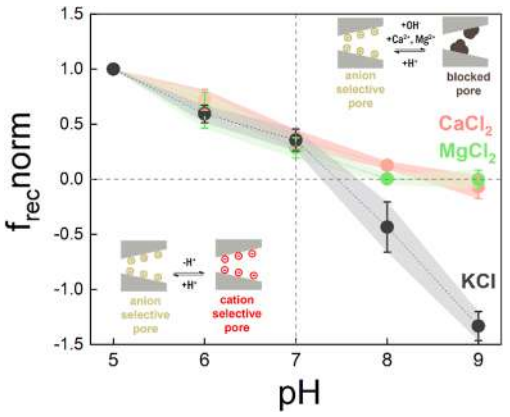

Figure 1. Normalized rectification efficiency vs pH of the urease−PAH−PET nanochannels. Curves were measured in the electrolyte solution (0.1 M KCl) (black dot) and 10 mM $CaCl_2$ (red dot) or 10 mM $MgCl_2$ (green dots). In all cases, the pH was adjusted with the dropwise addition of NaOH or HCl to reach each pH value. n = 3 technical replicates (mean ± SD).

f_{rec}norm with pH when 10 mM $MgCl_2$ is added to the electrolyte solution. Similar behavior is observed with $MgCl_2$ and $CaCl_2$ at all pH values. Particularly at pH values higher than 7, no inversion of rectification is observed, as expected when nanoprecipitation occurs.

To study the possibility of applying nanoprecipitation as a reaction that controls reconfigurable nanofluidic circuits and improves the sensitivity of the nanofluidic architecture, we included Ca^{2+} ions in the electrolyte solution when sensing urea with urease−PAH−PET nanochannels (Scheme 1). Figure 2a shows the I vs V curves of a nanochannel modified with urease−PAH in the presence of the electrolyte solution and when 10 mM Ca^{2+} is added, in both cases at pH 5 and in the absence of urea. No significant change is observed between these two cases. Then, if 10 mM urea is added to the electrolyte solution at pH 5, a huge change in the rectification properties is observed, including an inverse in the rectification direction (Figure 2a, from blue to red). As we previously reported,[18] when urea is present in the solution, the urease enzyme catalyzes the conversion of urea to ammonia and OH^- ions (Figure 2b), thereby producing a local increase in pH and the deprotonation of the amine group of the polymer. Thus, a change in the surface charge of the nanochannel is produced, and a change in the rectification properties is observed. However, we observed a different scenario when 10 mM urea was added to the electrolyte solution at pH 5, containing 10 mM $CaCl_2$. In this case, the current at positive potential decreases drastically, and there is no inversion in the direction of rectification. These results are in concordance with the results shown in Figure 1, where at pH values higher than 7, f_{rec}s are always close to 1. This indicates that a high concentration of urea can produce a significant increase in the local pH, and when the pH is higher than 7, the nanoprecipitation reaction can take place (Figure 2b).

Moreover, we also investigated the reversibility of the nanofluidic biosensor with the addition of Ca^{2+}. We were interested in assessing whether the system was still responsive after exposure to high concentrations of urea in the presence of Ca^{2+} ions. Thus, we performed experiments by successively changing the electrolyte solution from a 0.1 M KCl solution to a 10 mM urea +10 mM Ca^{2+} in a 0.1 M KCl solution, which is close to the saturation region. I vs V curves were measured for each cycle, and the rectification factors were calculated and plotted successively (Figure 3). We performed 3 repetition

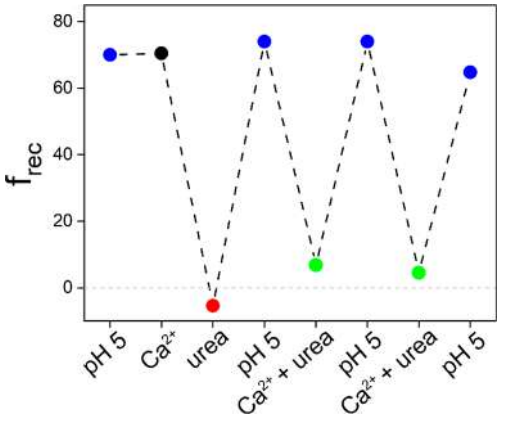

Figure 3. Reversibility tests for a urease−PAH-modified nanochannel. f_{rec} was obtained for urease−PAH-modified nanochannels for successive electrolyte solution changes.

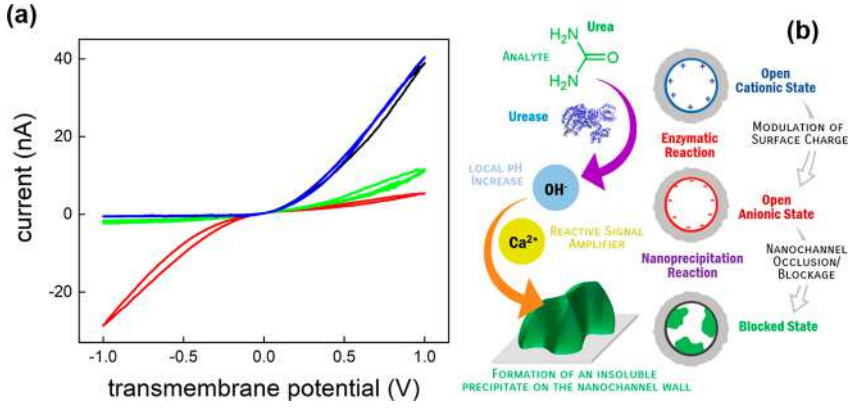

Figure 2. (a) Current−voltage curves measured of the urease−PAH−PET nanochannels in different electrolyte solutions: 0.1 M KCl pH = 5 (blue); 10 mM $CaCl_2$ and 0.1 M KCl pH = 5 (black); 10 mM urea and 0.1 M KCl pH = 5 (red); and 10 mM $CaCl_2$, 10 mM urea, and 0.1 M KCl pH = 5 (green). (b) Representation of the different processes taking place in the enzymatic nanofluidic biosensor when the device is exposed to the analyte.

https://doi.org/10.1021/acs.analchem.4c00203
Anal. Chem. 2024, 96, 5282−5288

cycles, and the biosensor did not lose its responsive behavior, thus implying that the nanoprecipitation reaction is reversible, as reported by previous modeling articles. Using theoretical modeling based on Poisson−Nernst−Planck equations, it was reported that the precipitate would dissolve inside the nanopore.[22] Moreover, molecular dynamics simulations propose an alternative mechanism where the entire precipitate exits the pore after being released from the nanopore surface. These simulations showed that the precipitate remains strongly attached to carboxyl groups. However, by reprotonation of the PET carboxyl groups exposed in the nanopore, the precipitate can detach from the PET surface and diffuse out of the pore, leaving the pore open and restoring ion flow.[24] With both mechanisms, upon returning to pH 5, the nanopore surface charge and exclusion volume are restored.

Furthermore, we studied the kinetic response of a urease−PAH−PET nanochannel by the addition of 1 mM urea while measuring the transmembrane current at 1 V in the presence of 10 mM $CaCl_2$ in the electrolyte solution. Information regarding how fast the system responds to the presence of the stimulus in solution is an important aspect of reconfigurable systems. Figure 4 shows a steep decrease in the current immediately after the addition of urea and stabilization at a lower current within a few minutes.

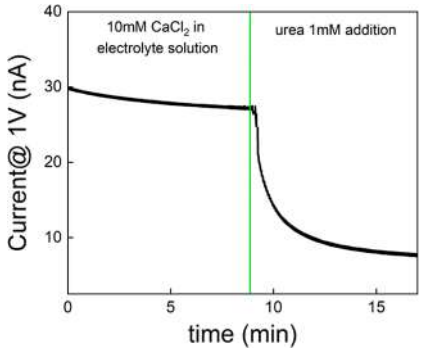

Figure 4. Kinetic response of a urease/PAH/PET nanochannel to the addition of 1 mM urea while measuring the transmembrane current at 1 V.

The effect of nanoprecipitation on the analytical performance of nanochannel-based sensors was studied by analyzing how the f_{rec}norm changes with different concentrations of urea. Figure 5 shows the dependence of the f_{rec}norm with urea concentration for urease−PAH−PET nanochannels in the presence of the electrolyte solution at pH 5 (black) and when 10 mM Ca^{2+} (red) or Mg^{2+} (green) is added. When the divalent cations are added to the solution, three main effects are observed. First, as described previously, at a high concentration of urea, no inversion in the f_{rec}norm is observed. Second, there is a shift in the dynamic linear range to lower concentrations in the presence of the divalent cation, producing a lower detection limit in the sub-nM range, 1 order of magnitude lower than without them. Furthermore, with Mg^{2+}, the shift in the dynamic range to lower concentrations is a little higher than that with Ca^{2+}. This differences can be explained by the lower K_{ps} of Mg^{2+} than Ca^{2+} precipitate [K_{sp} $Ca(OH)_2 = 5 \times 10^{-6}$ vs K_{sp} $Mg(OH)_2 = 1 \times 10^{-11}$]. Third, the slope of the f_{rec}norm vs urea concentration curve is higher when divalent cations are added (-0.32 ± 0.01 for Mg^{2+} and -0.43 ± 0.02 for Ca^{2+}) than without them (-0.23 ± 0.02), thus the sensitivity of the sensor is higher when divalent cations are added. It is interesting to note that the sensitivity is only up to two times higher when divalent cations are added compared with adding just K^+ ions. Moreover, we observed that the sensitivity of Mg^{2+} is a little lower than Ca^{2+}, contrary to what we could expect based on the K_{sp}. Then, these observations can indicate that the enzymatic reaction and not the nanoprecipitation reaction has a major impact on the sensitivity, while the nanoprecipitation reaction has a major impact on modulating the dynamic range and detection limit of the sensor.

These results show that it is possible to tune the dynamic range of the sensor by controlling the nanoprecipitation reaction inside the nanopore. By simply adding a divalent cation to the electrolyte solution, it is possible to quantify 1-fold lower concentrations of urea, being able to detect in the sub-nM range.

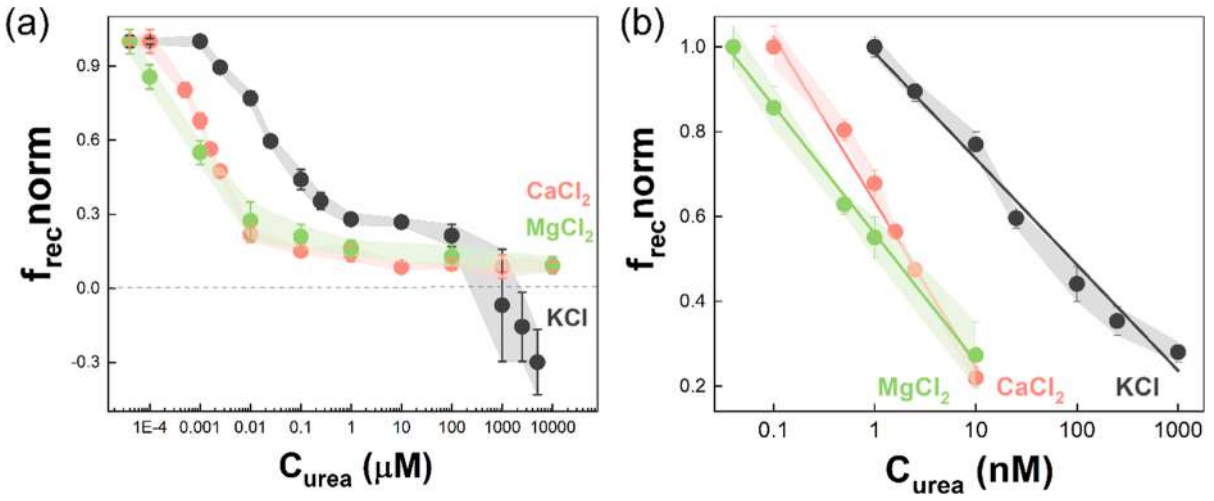

Figure 5. (a) Dependence of the f_{rec}norm with urea concentration in the presence of electrolyte solution (0.1 M KCl pH = 5, black) and when 10 mM Ca^{2+}(red) or Mg^{2+}(green) is added to the electrolyte solution. (b) Linear dynamic range with and without Ca^{2+} or Mg^{2+}. The error bar corresponds to 3 independent measurements for each concentration of urea (mean ± SD).

https://doi.org/10.1021/acs.analchem.4c00203
Anal. Chem. 2024, 96, 5282−5288

CONCLUSIONS

Overall, we have demonstrated that the nanoprecipitation reaction inside nanochannels works as a "reactive signal amplifier," providing a simple tool to improve the detection limit of nanopore-based sensors (subnanomolar detection of small molecules) and allowing tuning the dynamic lineal range of small molecule targets, as exemplified here with urea. We have shown that the precipitation of the insoluble product in the presence of the target analyte allows the occlusion of the nanofluidic nanochannel with a concomitant effect on the iontronic signal. Thus, the nanoprecipitation process provides a valuable strategy for amplifying the detection process. Other authors have employed biocatalyzed precipitations of insoluble products as a strategy to amplify electrochemical or microgravimetric sensing methods, such as chronopotentiometry, Faradaic impedance spectroscopy, or quartz crystal microbalance detection.[31−34] Different from previous approaches, we have used enzymatically induced nanoprecipitation in the presence of reactive signal amplifiers as a method to amplify/enhance the iontronic transduction of the biorecognition process in the nanochannel, i.e., the nanofluidic transducers. We also demonstrated that this approach not only enables a qualitative determination of the analyte but also the quantitative correlation between the iontronic signal and the analyte concentration. In the particular case of nanofluidic urea detection, we have shown that this approach leads to an improvement of an order of magnitude in the detection limit, from the nM range to the sub-nM range. This approach, based on concerted functions including pH-shifting enzymatic activity and nanoprecipitation, could potentially be applied to other enzymatic systems that induce a localized pH increase as a result of the enzymatic process. Given an enzymatic system that leads to a pH elevation in the presence of the analyte, once the enzyme is integrated within the nanochannel, the nanofluidic system would produce an amplified iontronic response when the enzymatic process takes place in the presence of Mg^{2+} or Ca^{2+} ions.

In addition to the nanofluidic sensing capabilities of the nanoprecipitation process, this work shows the use of divalent cations as a strategy to design chemically reconfigurable nanofluidic circuits that have the advantage of being reversible and with a fast response. In this context, we envision that the incorporation of integrated molecular systems displaying concerted functions inside nanochannels could turn into an enabling technology, leading to the production of nanofluidic biosensors with optimized properties.

ASSOCIATED CONTENT

Supporting Information

The Supporting Information is available free of charge at https://pubs.acs.org/doi/10.1021/acs.analchem.4c00203.

Additional materials, including I vs V curves of the modified nanopores at different pH values (PDF)

AUTHOR INFORMATION

Corresponding Authors

Ana S. Peinetti − *INQUIMAE (CONICET)—Departamento de Química Inorgánica, Analítica y Química Física, Facultad de Ciencias Exactas y Naturales, Universidad de Buenos Aires, C1428EHA Buenos Aires, Argentina*;
Email: apeinetti@qi.fcen.uba.ar

Omar Azzaroni − *Instituto de Investigaciones Fisicoquímicas Teóricas y Aplicadas (INIFTA), Departamento de Química, Facultad de Ciencias Exactas, Universidad Nacional de La Plata (UNLP), CONICET, 1900 La Plata, Argentina*;
orcid.org/0000-0002-5098-0612;
Email: omarazzaroni@quimica.unlp.edu.ar; https://softmatter.quimica.unlp.edu.ar

Authors

M. Lorena Cortez − *Instituto de Investigaciones Fisicoquímicas Teóricas y Aplicadas (INIFTA), Departamento de Química, Facultad de Ciencias Exactas, Universidad Nacional de La Plata (UNLP), CONICET, 1900 La Plata, Argentina*

Maria Eugenia Toimil-Molares − *GSI Helmholtzzentrum für Schwerionenforschung, 64291 Darmstadt, Germany; Technische Universitat Darmstadt, 64287 Darmstadt, Germany*

Complete contact information is available at: https://pubs.acs.org/10.1021/acs.analchem.4c00203

Author Contributions

The manuscript was written through the contributions of all authors. All authors have given approval to the final version of the manuscript.

Funding

This study was supported by the initiative and networking fund of the Helmholtz Association of German Research Centers under the CORAERO Project (grant KA1-Co-06). The authors also acknowledge financial support from CONICET and ANPCyT (PICT-2020-02468).

Notes

The authors declare no competing financial interest.

ACKNOWLEDGMENTS

This study was supported by the Initiative and Networking Fund of the Helmholtz Association of German Research Centers under the CORAERO Project (grant KA1-Co-06). The results presented here are based on a UMAT irradiation experiment, which was performed at the beamline X0 at the GSI Helmholtzzentrum für Schwerionenforschung, Darmstadt (Germany) in the frame of FAIR-Phase 0. O. A. gratefully acknowledges funding from the Georg Forster Award of the Alexander von Humboldt Foundation.

REFERENCES

(1) Siwy, Z. S. *Adv. Funct. Mater.* **2006**, *16* (6), 735−746.
(2) Gilles, F. M.; Tagliazucchi, M.; Azzaroni, O.; Szleifer, I. *J. Phys. Chem. C* **2016**, *120* (9), 4789−4798.
(3) Zhu, Z.; Wang, D.; Tian, Y.; Jiang, L. *J. Am. Chem. Soc.* **2019**, *141* (22), 8658−8669.
(4) Aluru, N. R.; Aydin, F.; Bazant, M. Z.; Blankschtein, D.; Brozena, A. H.; de Souza, J. P.; Elimelech, M.; Faucher, S.; Fourkas, J. T.; Koman, V. B.; Kuehne, M.; Kulik, H. J.; Li, H.-K.; Li, Y.; Li, Z.; Majumdar, A.; Martis, J.; Misra, R. P.; Noy, A.; Pham, T. A.; Qu, H.; Rayabharam, A.; Reed, M. A.; Ritt, C. L.; Schwegler, E.; Siwy, Z.; Strano, M. S.; Wang, Y.; Yao, Y.-C.; Zhan, C.; Zhang, Z. *Chem. Rev.* **2023**, *123* (6), 2737−2831.
(5) Song, M.; Sun, Z.; Han, C.; Tian, D.; Li, H.; Jiang, L. *Chem.—Eur. J.* **2014**, *20* (26), 7987−7993.
(6) Pérez-Mitta, G.; Toimil-Molares, M. E.; Trautmann, C.; Marmisollé, W. A.; Azzaroni, O. *Adv. Mater.* **2019**, *31* (37), 1901483.
(7) Xiao, K.; Wan, C.; Jiang, L.; Chen, X.; Antonietti, M. *Adv. Mater.* **2020**, *32*, 2000218.

(8) Laucirica, G.; Terrones, Y. T.; Cayón, V.; Cortez, M. L.; Toimil-Molares, M. E.; Trautmann, C.; Marmisollé, W.; Azzaroni, O. *Trac. Trends Anal. Chem.* **2021**, *144*, 116425.
(9) Zhang, Z.; Wen, L.; Jiang, L. *Nat. Rev. Mater.* **2021**, *6* (7), 622−639.
(10) Su, Y.-S.; Hung, W.-H.; Fauziah, A. R.; Siwy, Z. S.; Yeh, L.-H. *Chem. Eng. J.* **2023**, *456*, 141064.
(11) Wang, J.; Zhou, Y.; Jiang, L. *ACS Nano* **2021**, *15* (12), 18974−19013.
(12) Liu, L.; Luo, C.; Zhang, J.; He, X.; Shen, Y.; Yan, B.; Huang, Y.; Xia, F.; Jiang, L. *Small* **2022**, *18* (37), 2201925.
(13) Huang, Y.; Liu, L.; Luo, C.; Liu, W.; Lou, X.; Jiang, L.; Xia, F. *Chem. Soc. Rev.* **2023**, *52* (18), 6270−6293.
(14) Pérez-Mitta, G.; Albesa, A.; Gilles, F. M.; Toimil-Molares, M. E.; Trautmann, C.; Azzaroni, O. *J. Phys. Chem. C* **2017**, *121* (16), 9070−9076.
(15) Laucirica, G.; Pérez-Mitta, G.; Toimil-Molares, M. E.; Trautmann, C.; Marmisollé, W. A.; Azzaroni, O. *J. Phys. Chem. C* **2019**, *123* (47), 28997−29007.
(16) Fink, D.; Hernandez, G. M.; Alfonta, L. *Sens. Actuators, B* **2011**, *156* (1), 467−470.
(17) Hou, G.; Zhang, H.; Xie, G.; Xiao, K.; Wen, L.; Li, S.; Tian, Y.; Jiang, L. *J. Mater. Chem. A* **2014**, *2* (45), 19131−19135.
(18) Pérez-Mitta, G.; Peinetti, A. S.; Cortez, M. L.; Toimil-Molares, M. E.; Trautmann, C.; Azzaroni, O. *Nano Lett.* **2018**, *18* (5), 3303−3310.
(19) Litvinchuk, S.; Tanaka, H.; Miyatake, T.; Pasini, D.; Tanaka, T.; Bollot, G.; Mareda, J.; Matile, S. *Nat. Mater.* **2007**, *6* (8), 576−580.
(20) Terrones, Y. T.; Laucirica, G.; Cayón, V. M.; Fenoy, G. E.; Cortez, M. L.; Toimil-Molares, M. E.; Trautmann, C.; Mamisollé, W. A.; Azzaroni, O. *Chem. Commun.* **2022**, *58*, 10166−10169.
(21) Powell, M. R.; Sullivan, M.; Vlassiouk, I.; Constantin, D.; Sudre, O.; Martens, C. C.; Eisenberg, R. S.; Siwy, Z. S. *Nat. Nanotechnol.* **2008**, *3* (1), 51−57.
(22) Innes, L.; Powell, M. R.; Vlassiouk, I.; Martens, C.; Siwy, Z. S. *J. Phys. Chem. C* **2010**, *114* (18), 8126−8134.
(23) Cruz-Chu, E. R.; Schulten, K. *ACS Nano* **2010**, *4* (8), 4463−4474.
(24) Vilozny, B.; Actis, P.; Seger, R. A.; Pourmand, N. *ACS Nano* **2011**, *5* (4), 3191−3197.
(25) Siwy, Z. S.; Powell, M. R.; Petrov, A.; Kalman, E.; Trautmann, C.; Eisenberg, R. S. *Nano Lett.* **2006**, *6* (8), 1729−1734.
(26) Cruz-Chu, E. R.; Ritz, T.; Siwy, Z. S.; Schulten, K. *Faraday Discuss.* **2009**, *143*, 47−62.
(27) Powell, M. R.; Sullivan, M.; Vlassiouk, I.; Constantin, D.; Sudre, O.; Martens, C. C.; Eisenberg, R. S.; Siwy, Z. S. *Nat. Nanotechnol.* **2008**, *3* (1), 51−57.
(28) Pérez-Mitta, G.; Burr, L.; Tuninetti, J. S.; Trautmann, C.; Toimil-Molares, M. E.; Azzaroni, O. *Nanoscale* **2016**, *8* (3), 1470−1478.
(29) Pérez-Mitta, G.; Albesa, A.; Gilles, F. M.; Toimil-Molares, M. E.; Trautmann, C.; Azzaroni, O. *J. Phys. Chem. C* **2017**, *121* (16), 9070−9076.
(30) Brunsen, A.; Díaz, C.; Pietrasanta, L. I.; Yameen, B.; Ceolín, M.; Soler-Illia, G. J. A. A.; Azzaroni, O. *Langmuir* **2012**, *28* (7), 3583−3592.
(31) Patolsky, F.; Zayats, M.; Katz, E.; Willner, I. *Anal. Chem.* **1999**, *71* (15), 3171−3180.
(32) Alfonta, L.; Bardea, A.; Khersonsky, O.; Katz, E.; Willner, I. *Biosens. Bioelectron.* **2001**, *16* (9−12), 675−687.
(33) Jin, X.; Jin, X.; Liu, X.; Chen, L.; Jiang, J.; Shen, G.; Yu, R. *Anal. Chim. Acta* **2009**, *645* (1−2), 92−97.
(34) Akter, R.; Rahman, M. A.; Rhee, C. K. *Anal. Chem.* **2012**, *84* (15), 6407−6415.
(35) Apel, P. Y.; Blonskaya, I. V.; Dmitriev, S. N.; Orelovitch, O. L.; Presz, A.; Sartowska, B. A. *Nanotechnology* **2007**, *18* (30), 305302.
(36) Apel, P. Y.; Bashevoy, V. V.; Blonskaya, I. V.; Lizunov, N. E.; Orelovitch, O. L.; Trautmann, C. *Phys. Chem. Chem. Phys.* **2016**, *18* (36), 25421−25433.

https://doi.org/10.1021/acs.analchem.4c00203
Anal. Chem. 2024, 96, 5282−5288